Cite this: DOI: 10.1039/c0xx00000x

www.rsc.org/xxxxxx

ARTICLE TYPE

Synthesis of vertical aligned TiO_2@polyaniline core-shell nanorods for high-performance supercapacitors

Li Zhang,[a] Lei Chen,[b] Bin Qi,[a] Guocheng Yang,[c] Jian Gong*[a]

Received (in XXX, XXX) Xth XXXXXXXXX 200X, Accepted Xth XXXXXXXXX 200X
DOI: 10.1039/b000000x

The orderd arrays of TiO_2@polyaniline core-shell nanocomposite that exhibits relatively higher electrochemical property with as high as 820 F g^{-1} at 1 A g^{-1} is prepared by the combination of hydrothermal and in situ chemical polymerization methods. The specific capacitance retention of the nanocomposite is over 85 % after 1000 cycles of charge and discharge at the current density of 10 A g^{-1}, suggesting the good cycling stability.

For supercapacitors (SCs), it is important to choose a suitable electrode material with high capacity performance. As one knows, carbon materials, noble metal oxides, and conducting polymers are the three main types of greatly investigated electrode materials.[1] Among them, noble metal oxide and conducting polymer have shown to deliver higher specific capacitance than carbon materials, since they store charge through both double-layer and redox capacitive mechanisms.[2-4] Compared with noble metal xoide, conducting polymers, such as polyaniline (PANI), offer more potential applications for solving energy crisis and enviromnental pollution because of their high conductivity and capacitance, low cost, easy synthesis and good stability. However, as a kind of SCs materials, PANI shows an obvious volume change during the charge and discharge process, which has largely decreased its mechanical stability during use.[5] For the reason given above, the cycling stability is usual poor, which has become a major obstacle for PANI to be used in supercapacitors.

In order to solve the poor cyclability of PANI, a good and effective method to add inorganic support materials in PANI has been demonstrated.[6-9] Among these inorganic support materials, TiO_2 has been widely used and investigated because of its lower cost, environmental-friendly nature, and good adhesion between PANI and fluorine-doped tin oxide (FTO) substrate. Recently, C. Q. Bian *et al*. reported on a TiO_2/PANI fibriform composite in which the nano-TiO_2 particles were embeded within the PANI fibers.[10] The specific capacitance of the as-prepared composite was up to 330 F/g at a constant current density of 1.5 A g^{-1}. X. W. Li *et al.* prepared a highly homogeneous TiO_2/PANI hybrid by the oxidative polymerization of aniline with the simultaneous hydrolysis of $Ti(SO_4)_2$.[11] Its initial specific capacitance is about 495 F g^{-1}, and its capacitance retention ratio reaches 50 % after 3000 consecutive cycles. K. Y. Xie *et al.* obtained a novel composite electrode made of PANI nanowire-titania nanotube array via electropolymerizing aniline onto an anodized titania nanotube array.[12] The specific capacitance was as high as 732 F g^{-1} at 1 A g^{-1}. The cycle life was maintained with a retention of 86 % of the initial specific capacitance after 2000 cycles.

Following our extensive explorations of PANI materials,[13-17] in this communication, we report an easy method for the synthesis of a TiO_2@PANI core-shell nanocomposite with well-defined vertical aligned morphologies. An excellent specific capacitance of as high as 820 F g^{-1} at a charge and discharge current density of 1 A g^{-1} was obtained, which is the highest capacitance reported to date for TiO_2@PANI materials. After 1000 cycles, the specific capacitance retention is over 85 %.

A typical fabrication procedure is shown in Scheme 1. TiO_2 nanorods grown on the FTO substrate were prepared first by the reported hydrothermal method.[18] Then, carbon-coated TiO_2 (TiO_2@C) nanorods were obtained according to a similar approach to the previous report.[19] For the synthesis of TiO_2@C nanorods, the TiO_2 nanorods on the FTO substrate were immersed into a 30 mL of glucose solution (0.3 mol L^{-1}) for 12 h. The free space between neighboring nanorods would allow adsorption of glucose molecules onto the nanorod surface. After that, the FTO substrate with the TiO_2 nanorods was taken out, dried and further annealed in Ar gas at 500 °C for 5h to allow the carbonization of glucose. In the end, a layer carbon could be painted homogenously on the surface of the TiO_2 nanorods. In order to get the final TiO_2@PANI core-shell nanorods, the TiO_2@C nanorods were immersed into a 12 mL of $KMnO_4$.

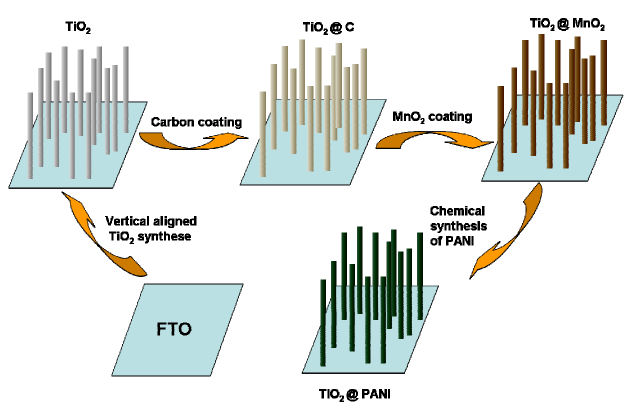

Scheme 1 Schematic illustration of the fabrication process for designed vertical aligned TiO_2@PANI core–shell nanocomposite electrode

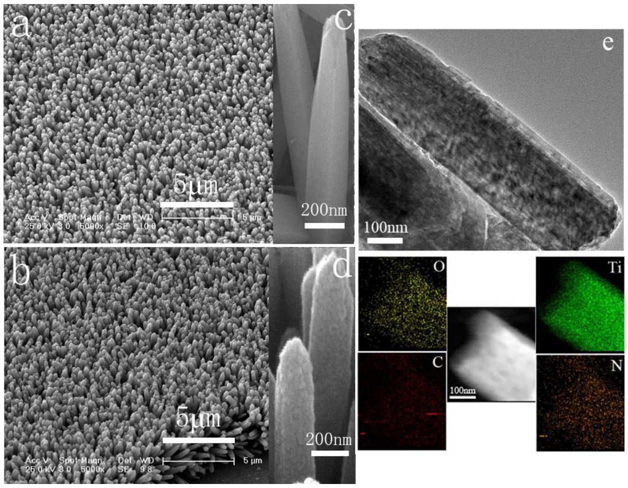

Fig.1 SEM images of TiO_2 nanorods (a, c) and TiO_2@PANI core-shell nanocomposite (b,d). TEM image of TiO_2@PANI core-shell nanocomposite, and elemental maps of O, Ti, C and N for TiO_2@PANI (e)

solution (0.03 mol L^{-1}) and sealed in a Teflon-lined stainless steel autoclave at 160 °C for 5 h. Due to the interfacial reaction between C and $KMnO_4$, TiO_2@MnO_2 core-shell nanorods were obtained. At last, 0.2 mL of aniline was added into the 30 mL of HCl solution (1 mol L^{-1}) with stiring for 5 min. Then the FTO with TiO_2@MnO_2 core-shell nanorods was immersed into the above solution. The MnO_2 served as the oxidant for the synthesis of PANI. After reacting for 12 h at 0-5 °C, the dark green TiO_2@PANI core-shell nanorods was obtained. Detailed preparation and characterization of TiO_2, TiO_2@C, TiO_2@MnO_2, and TiO_2@PANI nanorods can be found in EIS†.

Fig. 1 shows Scanning electron microscopy (SEM) images of the TiO_2 nanorods (Fig.1a, c) and the TiO_2@PANI core-shell nanorods (Fig. 1b, d). The low magnification SEM image of TiO_2 nanorods (Fig.1a) shows that the TiO_2 nanorods as the core are uniform and with average diameter in the range of about 180-250 nm. The higher magnification SEM of TiO_2 nanorods (Fig.1c) shows that the walls are relatively smooth, but the tip of them are relatively rough. After coated with PANI shell, as shown in Fig.1b, the nanocomposite of TiO_2@PANI is also uniform, and in Fig.1d, the higher magnification SEM image of TiO_2@PANI shows that it is more rougher than the core TiO_2, which is also supported by transmission electron microscopy (TEM) images (Fig. 1e) of the TiO_2@PANI nanocomposite. A core-shell nanostructure is very obvious, and the TEM image of the TiO_2@PANI core-shell nanorods shows that the thickness of the PANI shell is about 45-50 nm. The distribution of PANI on the TiO_2 nanorods is investigated by STEM-EDX elemental mapping. The bottem of Fig.1e shows that C (referring to as C from PANI) is distributed similarly as Ti (referring to TiO_2) and N (in PANI), O (in TiO_2), indicating that a uniform PANI film is produced on the surface of TiO_2. X-ray diffraction (XRD) patterns, Fourier transforms infrared spectrum (FT-IR), and Energy-dispersive X-ray analysis (EDX) were also used to characterize the TiO_2, TiO_2@C, TiO_2@MnO_2 and TiO_2@PANI core-shell nanorods. (Fig. S1, S2 and S4 in EIS†). At the same time, the morphologies of TiO_2@C, TiO_2@MnO_2 and TiO_2@PANI and pure PANI are shows in EIS†. (Fig. S3)

Cyclic voltammetry (CV) test was aimed to study the electrochemical properties of nanocomposite electrode and the galvanostatic charge-discharge (GCD) test was used to demonstrate the capacitive behavior of the vertical aligned TiO_2@PANI nanocomposite. In Fig. 2a, the CV curves of the vertical aligned TiO_2@PANI core-shell nanorods and pure TiO_2 nanorods measured at the scan rate of 5 mV s^{-1} are distinctly different. From the measured results, we can see that the CV curve of the TiO_2@PANI core-shell nanorods shows two pairs of redox peaks of PANI. The first pair of redox peaks is attributed to redox transition of PANI from leucoemeraldine to emeraldine states, and the other pair of peak is ascribed to the transformation from emeraldine to pernigraniline states.[20] The CV curve of the TiO_2 nanorods shows a typical electric double layer capacitance. Fig. 2b showed the CV curves of the TiO_2@PANI electrode at different scan rates of 5, 10, 20, 50 and 100 mv s^{-1}, respectively. It is obvious that the shape of the CV curves doesn't change evidently below 20 mV/s. And the total peak current density increases with the increase of scan rate, which demonstrates a good rate property and excellent capacitance of the TiO_2@PANI electrode.[21] Meanwhile, the current intensity of the redox peaks increase with increasing voltage, indicating an increased resistance of the electrode materials.[22]

Fig. 3a shows galvanostatic discharge (GCD) curves of the TiO_2@PANI electrode at different current densities. The specific capacitance values were evaluated from discharge curves, that the detail calculation equations about the electrodes were listed in EIS†. The specific capacitance of the TiO_2@PANI nanocomposite is as high as 820 F g^{-1} at a charge and discharge current density of 1A g^{-1}, and corresponding energy density and power density are of 102.5 Wh kg^{-1} and 4.62 kw kg^{-1}.

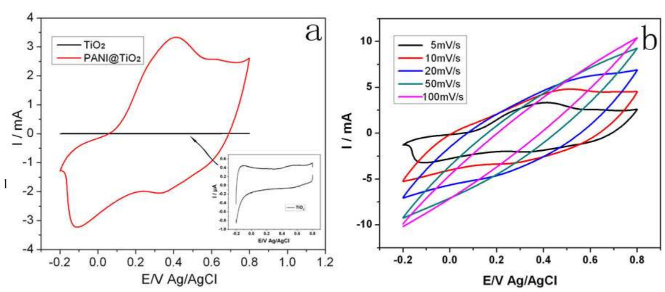

Fig. 2 (a) CV curves of the TiO_2@PANI core-shell nanorods and TiO_2 nanorods at a scan rate of 5 mV s^{-1}. The inset is the enlarged CV curve of TiO_2 nanorods. (b) CV curves of the TiO_2@PANI core-shell nanorods at different scan rate of 5, 10, 20, 50 and 100 mV s^{-1}.

In order to improve our TiO_2@PANI core-shell nanorods has the best electrochemical performance than other products, We conducted the comparison of TiO_2@C, TiO_2@MnO_2, PANI and TiO_2@PANI with CV and GCD test, (in EIS†. Fig. S5 and S6). As a result, we confirm that the TiO_2@PANI has the best performance among them.

Cycling stability is another important factor to determine the practical applications of SCs. The electrochemical stability of the

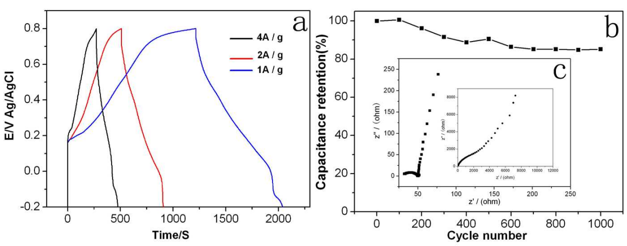

Fig. 3. (a) The GCD curves of vertical aligned TiO_2@PANI core-shell nanorods at different current densities of 1, 2 and 4 A g^{-1}. (b) Variation of the specific capacitance of the TiO_2@PANI core-shell nanorods as a function of the cycle number. (c) Nyquist plot of the TiO_2@PANI nanocomposite electrode in a frequency range of 0.01 Hz to 100 kHz (the perturbation amplitude is 5 mV). The inset shows the plot of TiO_2.

TiO_2@PANI electrode, consecutive charge–discharge cycles were measured at a current density of 10 A g^{-1} (Fig. 3b). The TiO_2@PANI electrode was shown to keep 85 % of its initial capacitance after 1000 cycle tests, suggesting that the TiO_2@PANI electrode exhibits excellent long-term cycle ability and a high degree of reversibility in consecutive charge–discharge cycles. We also provided the morphology of the TiO_2@PANI core-shell nanorod. (EIS† Fig. S7), we can see from it that the TiO_2@PANI nanorod hasn't change very obviously. Compared with the reported studies, it is obvious that the presence of well-orderd TiO_2 arrays as a support for PANI is also very advantageous to reduce the electrochemical degradation of PANI and improve its cycle ability as electrode material.

For energy storage devices, It is important for

To further differentiate the supercapacitor based on the vertical aligned TiO_2@PANI core-shell nanorods, we tested the charge transport and ion diffusion of the composite by using electrochemical impedance spectroscopy (EIS). Nyquist plot was generated as shown in Fig. 3c. From the Nyquist plot of both the TiO_2@PANI and the TiO_2 nanorods consist of a semicircle in high-to-medium frequency region and an inclined line in low-frequency region. The semicircle corresponds to the charge-transfer impedance on electrode/electrolyte interface, and the inclined line in low frequency region is assigned to the ion diffusion process within electrodes.[23] Compared with the TiO_2 nanorods, the diameter of the semicircle for the vertical aligned TiO_2@PANI core-shell nanorods is much smaller, revealing a greatly reduced charge-transfer resistance (Rct). The reduce of Rct should be ascribe to the large surface area and prominently improved conductivity of the vertical aligned TiO_2@PANI core-shell nanorods. Moreover, in the low frequency regime, the EIS spectrum of the TiO_2@PANI core-shell nanorods exhibits a more vertical straight line along the imaging axis, which indicates a lower diffusion resistance in the electrode.

The more outstanding electrochemical performance of the vertical aligned TiO_2@PANI core-shell nanorods can be explained. Except the special synergistic effect of both components, the excellent performance of the nanocomposite also depends on the specific hierarchical architecture of the aligned TiO_2@PANI core-shell nanorods. Firstly, vertical PANI nanorods greatly increase the specific surface area of the nanocomposite, which benefits the ion diffusion from the bulky solution to the surface of the TiO_2@PANI core-shell nanorods. Therefore, the counterions can easily reach or leave the surface of the nanocomposite. Secondly, The counterions can penetrate the inner layer of the PANI and reach the surface and inner of the TiO_2, realizing the efficient utilization of the electrode materials.

In summary, the vertical aligned TiO_2@PANI core-shell nanorods were prepared by the combination of hydrothermal and *in situ* chemical polymerization methods. The orderd arrays of TiO_2@PANI core-shell nanorods so fabricated were found to exhibit relatively higher electrochemical property with an electrochemical capacitance. The specific capacitance was as high as 820 F g^{-1} at 1A g^{-1}. And, the specific capacitance retention of the nanocomposite was over 85 % after 1000 cycles of charge and discharge at the current density of 10 A g^{-1}, suggesting the good cycling stability. The good electrochemical performance was not only due to the synergistic effect of both individual component but also attributed to the unique vertical aligned structure of the electrode material, which providing high surface area, fast diffusion path for ions and long-term cycle stability. It was expected that the TiO_2@PANI nanocomposte as electrode material with excelent capacitive properties would greatly promote their practical applications to the energy storge for supercapacitors. This study provides a facile approach to fabricate a hybrid hierarchical nanocomposite using conducting polymers and inorganic material, and also shows that the nanocomposite for application in energy storage owing to its special structure.

This work was supported by the Program for Changjiang Scholars and Innovative Research Team in University.

Notes and references

[a]*Key Laboratory of Polyoxometalates Science of Ministry of Education, Northeast Normal University, Changchun, Jilin, 130024, China; E-mail: gongj823@nenu.edu.cn*
[b] *School of environment, Northeast Normal University.*
[c] *School of Chemistry and life science,Changchun University of Technology,Changchun, Jilin,130012, China.*
†*Electronic Supplementary Information (ESI) available: General experimental and FT-IR, XRD, EDX spectra and detailed discussion. See DOI: 10.1039/b000000x/*

1. G. P. Wang, L. Zhang and J. J. Zhang, *Chem. Soc. Rev.*, 2012, **41**, 797.
2. C. C. Hu, K. H. Chang, M. C. Lin and Y. T. Wu, *Nano Lett.*, 2006, **6**, 2690.
3. Z. L. Wang, R. Guo, G. R. Li, H. L. Lu, Z. Q. Liu, F. M. Xiao, M. Q. Zhang and Y. X. Tong, *J. Mater. Chem.*, 2012, **22**, 2401.
4. K. R. Prasad, K. K .Miura, *Chem.Mater.*, 2004, **16**, 1845.
5 B. K. Kuila, B. Nandan, M. Bohme, A. Janke and M. Stamm, *Chem. Commun.*, 2009, 5749..
6. X. M. Feng, R. M. Li, Y. W. Ma, R. F. Chen, N. E. Shi, Q. L. Fan and W. Huang, *Adv. Funct. Mater.* 2011, **21**, 2989.
7. Jaidev, R. I. Jafri, A. K. Mishra and S. Ramaprabhu, *J. Mater. Chem.*, 2011, **21**, 17601.
8. K. Wang, Q. H. Meng, Y. J. Zhang, Z. X. Wei and M. H. Miao, *Adv. Mater*. 2013, **25**, 1494.
9. S. H. Mujawar, S. B. Ambade, T. Battumur, R. B. Ambade and S. H. Lee, *Electrochim Acta*, 2011, **56**, 4462.
10. C. Q. Bian, A. Yu and H. Q. Wu, *Electrochem. Commun.*, 2009, **11**, 266.
11. X. W. Li, H. Zhang, G. C. Wang and Z. H. Jiang, *J. Mater. Chem.*, 2010, **20**, 10598.
12. K. Y. Xie, J. Li, Y. Q. Lai, Z. A. Zhang, Y. X. Liu, G.. G. Zhang and H. T. Huang, *Nanoscale*, 2011, **3**, 2202.

13. S. X. Yang, H. Y. Yang, H. Y. Ma, S. Guo, F. Cao, J. Gong and Y. L. Deng, *Chem.Commun.*, 2011, **47**, 2619.
14. S. X. Yang, X. J. Cui, J. Gong and Y. L. Deng, *Chem.Commun.*, 2013, **49**, 4676.
15. S. X. Yang, J. Gong and Y. L. Deng, *J. Mater. Chem.*, 2012, **22**, 13899..
16. S. X. Yang, J. Gong and Y. L. Deng, *J. Mater. Chem.*, 2012, **22**, 24522.
17. L. Zhang, H. Y. Ma, Fei Cao, Jian Gong and Z. M. Su, *J. Polym. Sci. Part A: Polym. Chem.* 2012, **50**, 912.
18. B. Liu and E. S. Aydil, *J. Am. Chem. Soc.* 2009, **131**, 3985.
19. X. Sun, Q. Li,Y. N. Lu and Y. B. Mao, *Chem. Commun.*, 2013, **49**, 4456.
20. C. C. Hu and J. Y. Lin, *Electrochim. Acta.*, 2002, **47**, 4055.
21. H. S. Fan, H. Wang, N. Zhao, X. L. Zhang and J. Xu, *J. Mater. Chem.*, 2012, **22**, 2774.
22. R. Montazami, V. Jain and J. R. Heflin, *Electrochim. Acta*, 2010, **56**, 990.
23. D. D. Zhu, Y. D. Wang, G. L. Yuan and H. Xia, *Chem. Commun.*, 2014, **50**, 2876.

Table of Contents

The orderd arrays of TiO_2@polyaniline core-shell nanocomposite that exhibits relatively higher electrochemical property with as high as 820 F g^{-1} at 1 A g^{-1} is prepared by a simple method. The specific capacitance retention of the nanocomposite is over 85 % after 1000 cycles of charge and discharge at the current density of 10 A g^{-1}.